Supplementary Information

Avrahami et al.,

Aging-dependent demethylation of regulatory elements correlates with chromatin state and improved β-cell function

Supplemental Experimental Procedures:

Pathway and motif analysis

The pathway analyses were generated through the use of Ingenuity Pathway Analysis (IPA; Ingenuity Systems, http://www.ingenuity.com) and DAVID for gene annotation (Dennis et al., 2003; Huang da et al., 2009a, b). De novo motif analyses were performed using HOMER (Heinz et al., 2010).

mRNA expression analysis

mRNA expression was measured using qRT–PCR, as previously described (Gupta et al., 2005). Primer sets can be found in the Supplemental Material (Table S7). RNA sequencing libraries were constructed from 200ng of total RNA isolated using the TruSeq RNA sample prep kit (Illumina). Single read sequencing was performed on Illumina hiSeq2000 to 100bp. Reads were aligned to the mouse genome mm9 using RUM (Grant et al., 2011). Read counts for RefSeq transcripts were processed with EdgeR (Robinson et al., 2010) to generate fold changes and p-values. P-values were converted to false discovery rates using the Benjamini & Hochberg mode of the R function p.adjust. Differentially-expressed genes were identified using an FDR threshold of 10%. mRNA levels were expressed in reads per kilobase of transcript per million mapped reads (RPKM).

ChIP analysis

ChIP and preparation of ChIP-Seq libraries was performed on sorted old and young mouse β cells as previously described (Bramswig et al., 2013), using antibody against H3K27ac (39685, Active Motif), H3K4me1 (ab8895, Abcam) and H3K27me3 (07-449, upstate). Paired-end sequencing was performed on the hiSeq2500 (50-bp reads) in rapid-run mode. Reads were

aligned to the genome using Bowtie (-k 1 -m 1–best–strata). Peaks were called using HOMER in histone mode and with PCR duplicates discarded. Regions were selected with a false discovery rate cutoff of 1% and STAR to determine enrichment of H3K27me3 (Lefterova et al., 2010).

Enhancer activity of beta cell–specific DMRs

DMRs associated with key genes of β cell function were cloned upstream of a luciferase gene and transiently transfected into MIN6 cells and HEK 293 cells to determine their possible activity as enhancers or silencers. Luciferase activity was normalized against the activity of a co-transfected Renilla construct, and mean values ± SEM are shown relative to empty vector (pGL4.23).

Islet insulin secretion

Islets were isolated from young (4-6 weeks old) and old (16 months) C57Bl6 mice using standard collagenase digestion followed by purification through a Ficoll gradient as previously described (Gupta et al., 2005). Following an overnight culture at 37°C, 150 islets were placed into a perifusion chamber (Millipore). To measure insulin release in response to glucose, islets were perifused with a 0-25mM glucose ramp and samples were collected at 1-min intervals for 120 minutes with a fraction collector (Waters Corporation). Insulin content was determined using a radioimmunoassay.

Assessment of old and young β cells function by single-cell glucose-stimulated calcium influx assay

Ca^{2+} imaging of dispersed islet cells retrieved from old (16 months) and young (4-6 weeks old) mice was carried out as previously described (Avrahami et al., 2014).

Human Islets

Human islets and relevant donor information including age, gender, and BMI were obtained from the Islet Cell Resource Center of the University of Pennsylvania, the NIDDK-supported Integrated Islet Distribution Program (iidp.coh.org), and the National Disease Research Interchange. Donor information is listed in Table S6.

Legends to Supplemental Figures:

Figure S1. Flow cytometry sorting of isolated pancreatic islet β cells of young and old mice. Related to Figure 1 (A) Pancreatic islets were isolated from young (4-6 weeks old) and old (16-20 months old) WT C57BL6 mice. Isolated islets were dissociated into single cells, stained using anti Insulin antibody (DAKO) and sorted by flow cytometry (FACS). P4, 98% pure β cell population. P3, non-beta islet cells (mainly alpha cells). (B) Flow cytometry sorting of live β cells from isolated pancreatic islets of young (4-6 weeks old) and old (16-20 months old) MIP-GFP mice for downstream RNA analyses.

Figure S2. Whole Genome Shotgun Bisulfite Sequencing (WGSBS) and ChIP-seq data of old and young β cells. Related to Figure 2 and 3. (A). Total number of reads, number of aligned reads and distribution of CpG coverage in the generated WGSB-Seq datasets representing Young and old β-cell populations. Sequencing statistics are also provided for H3K4me1, H3K27me3 and H3K27Ac ChIP-Seq and inputs of Young and old β-cell populations. (B) Comparison of CG and non-CG methylation in young and old β-cells. Most of the cytosine DNA methylation is present as expected, in the symmetrical CG sequences (black bars), while most cytosines in the symmetric and asymmetric contexts of CHG and CHH (where H is A, C or T, dark and light gray bars) are unmethylated. (C). Methylation levels of CpGs within specific genomic annotations show that promoters are largely unmethylated in β cells while the remainder of the genome is highly methylated, as previously reported in mouse intestinal epithelium (Sheaffer et al., 2014).

Figure S3. The methylome of old and young beta-cells. Related to Figure 2 and 3. (A,B), Distribution of UMRs, LMRs and FMRs among different genomic features in young (A) and old (B) β cells methylomes. In both methylomes, over 95% of the genome (FMRs, about 2.5 Gbp), is highly methylated. As expected, UMRs are highly enriched for gene promoters, encompassing 23.8 and 27.8 megabases in young and old β cells methylome respectively. Conversely, LMRs spanning an area of 79.5 and 70 megabases, respectively, are depleted of promoters and enriched for intergenic regions. (C-H), Genomic regions enriched for the active histone mark H3K27Ac

reside within LMRs and UMRs and occupy by β cell specific transcription factors. (C) Out of 9237 H4K27Ac peak calls distal to TSS, 98.5% reside within LMRs or UMRs. (D) Among 6515 H3K27Ac peaks near TSS, 100% reside within UMRs or LMRs. (E) 9% of all distal (≥1000bp from nearest TSS) UMRs and LMRs are enriched for H3K27Ac. (F) 40% of proximal (≤ 1000bp from nearest TSS) UMRs and LMRs are enriched for H3K27Ac. (G) Out of the 9% distal UMRs and LMRs enriched for H3K27Ac, 42% are bound by either Pdx1, NeuroD1, Foxa2 or any combination of these three β cell transcription factors. (H) Out of the 40% proximal UMRs and LMRs enriched for H3K27Ac, 27% are bound by either PDX1, NeuroD1, FOXA2 or any combination of these three β cell transcription factors.

Figure S4. β cell promoters, de novo methylated with aging, are enriched near genes involved in cell cycle control. Related to Figure 4. List of genes that display increased methylation in their promoter region and decreased expression with aging.

Figure S5. (A) Distribution of fold changes in RNA expression between young and old mouse β cells. Related to Figure 5. Histogram of statistically significant fold changes (FDR <= 10%) in RNA expression from RNASeq (black) compared to all fold changes regardless of statistical significance (gray). There are 4,040 down-regulated transcripts and 2,083 up-regulated transcripts. Fold changes for both directions are generally well in excess of 1.5x, but this is especially true for down-regulated genes. (B-C), Age-dependent downregulated and upregulated genes differ in their associated functional gene categories. Gene ontology analysis (DAVID (Dennis et al., 2003)) for genes that were found significantly repressed (B) or activated (C) by aging (FDR <= 10%, >2 fold change). Downregulated genes are enriched for developmental transcription factors and processes as well as biological pathways involving cell-cell signaling and proliferation. Upregulated genes are enriched for biological pathways essential for beta cell function such as protein processing and transport, mitochondrial activity and glucose metabolism.

Figure S6. Age-dependency of differential methylation of β cell enhancers is specific to β cells, and is not a general feature of all tissues. Related to Figure 6. (A-D), DMRs identified by whole genome bisulfite sequencing of young and old β cells and validated for enhancer

activity in MIN6 β cell line, were analyzed for their methylation levels in young versus old kidney and liver cells by targeted bisulfite sequencing. Three biological replicates of young and old Kidney and liver cells were used to verify methylation at the single-CpG level and regional average of a DMR associated with *Kcnj11*, encoding the Kir6.2 subunit of the ATP-sensitive potassium channel (A, kidney, B, liver) and a DMR associated with *Gck*, encoding glucokinase (C, kidney, D, liver). Both DMR regions decrease significantly in their regional average methylation with age in β-, but not kidney and liver cells (*Kcnj11*: 30.4% ± 15%; *Gck*: 21.3% ± 10.65%, $p < 0.01$ by t-test).

Titles of Supplemental Tables:

Supplemental Table S1: Related to figures 2 and 3. Title: List of significant DMRs, their distance from nearest gene, enrichment for H3K27Ac, H3K4me1, H3K27me3 and the beta cell TFs.

Supplemental Table S2A-H: Related to Figure 5. Title: List of activated and silenced genes with age and their associated DMRs.

Supplementary Table 3: Related to Figure 6. Title: List of DMRs analyzed for enhancer or silencer activity by luciferase assay.

Supplementary Table 4: Related to Figure 6 and S6. Title: Bisulfite-sequencing primers sequences.

Supplementary Table 5: Related to Figure 7. Title: List comparing the Age-related differential expression of key beta cell genes in human and mouse.

Supplementary table 6: Related to Figure 7. Title: Human islet donor information.

Supplementary Table 7: Related to Figure 7. Title: RT-qPCR primers sequences.

References

Avrahami, D., Li, C., Yu, M., Jiao, Y., Zhang, J., Naji, A., Ziaie, S., Glaser, B., and Kaestner, K.H. (2014). Targeting the cell cycle inhibitor p57Kip2 promotes adult human beta cell replication. The Journal of clinical investigation *124*, 670-674.

Bramswig, N.C., Everett, L.J., Schug, J., Dorrell, C., Liu, C., Luo, Y., Streeter, P.R., Naji, A., Grompe, M., and Kaestner, K.H. (2013). Epigenomic plasticity enables human pancreatic alpha to beta cell reprogramming. The Journal of clinical investigation *123*, 1275-1284.

Dennis, G., Jr., Sherman, B.T., Hosack, D.A., Yang, J., Gao, W., Lane, H.C., and Lempicki, R.A. (2003). DAVID: Database for Annotation, Visualization, and Integrated Discovery. Genome biology *4*, P3.

Grant, G.R., Farkas, M.H., Pizarro, A.D., Lahens, N.F., Schug, J., Brunk, B.P., Stoeckert, C.J., Hogenesch, J.B., and Pierce, E.A. (2011). Comparative analysis of RNA-Seq alignment algorithms and the RNA-Seq unified mapper (RUM). Bioinformatics *27*, 2518-2528.

Gupta, R.K., Vatamaniuk, M.Z., Lee, C.S., Flaschen, R.C., Fulmer, J.T., Matschinsky, F.M., Duncan, S.A., and Kaestner, K.H. (2005). The MODY1 gene HNF-4alpha regulates selected genes involved in insulin secretion. The Journal of clinical investigation *115*, 1006-1015.

Heinz, S., Benner, C., Spann, N., Bertolino, E., Lin, Y.C., Laslo, P., Cheng, J.X., Murre, C., Singh, H., and Glass, C.K. (2010). Simple combinations of lineage-determining transcription factors prime cis-regulatory elements required for macrophage and B cell identities. Molecular cell *38*, 576-589.

Huang da, W., Sherman, B.T., and Lempicki, R.A. (2009a). Bioinformatics enrichment tools: paths toward the comprehensive functional analysis of large gene lists. Nucleic acids research *37*, 1-13.

Huang da, W., Sherman, B.T., and Lempicki, R.A. (2009b). Systematic and integrative analysis of large gene lists using DAVID bioinformatics resources. Nature protocols *4*, 44-57.

Lefterova, M.I., Steger, D.J., Zhuo, D., Qatanani, M., Mullican, S.E., Tuteja, G., Manduchi, E., Grant, G.R., and Lazar, M.A. (2010). Cell-specific determinants of peroxisome proliferator-activated receptor gamma function in adipocytes and macrophages. Molecular and cellular biology *30*, 2078-2089.

Robinson, M.D., McCarthy, D.J., and Smyth, G.K. (2010). edgeR: a Bioconductor package for differential expression analysis of digital gene expression data. Bioinformatics *26*, 139-140.

Sheaffer, K.L., Kim, R., Aoki, R., Elliott, E.N., Schug, J., Burger, L., Schübeler, D., and Kaestner, K.H. (2014). DNA methylation is required for the control of stem cell differentiation in the small intestine. Genes & development *28*, 652-664.

Supplemental Figure S1

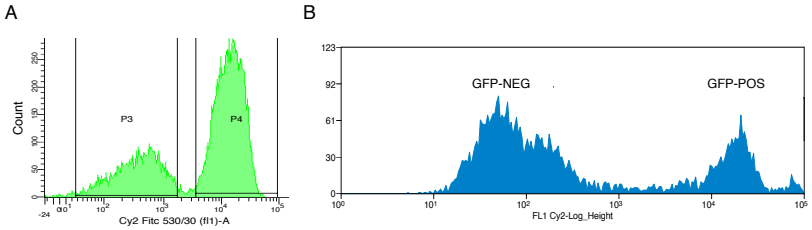

Supplemental Figure S2

A

WGSBS

Cell type	Sequenced Reads	Aligned Reads	Median coverage
Old β	533,126,025	515,174,774	18
young β	596,041,703	535,593,952	16

H3K4me1 ChIP-Seq

Cell type	Sequenced Reads	Aligned Reads	Alignment (%)
Young β input	27,871,399	20,617,705	73.97
Old β input	26,188,429	19,838,916	75.75
Old β H3K4me1	33,218,109	20,617,705	62.07
Young β H3K4me1	36,618,515	30,192,521	82.45

H3K27Ac ChIP-Seq

Cell type	Sequenced Reads	Aligned Reads	Alignment (%)
Young β input	65,725,153	41,929,794	63.80
Young β H3K27Ac	40,728,963	30,687,601	75.35

H3K27me3 ChIP-Seq

Cell type	Sequenced Reads	Aligned Reads	Alignment (%)
Young β input	111,357,319	85,885,472	77.13
Young β H3K27me3	65,226,664	45,598,233	69.91

B

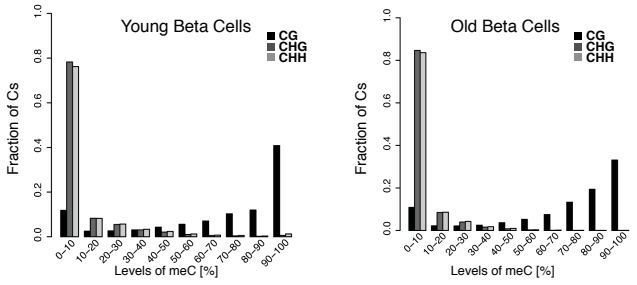

C

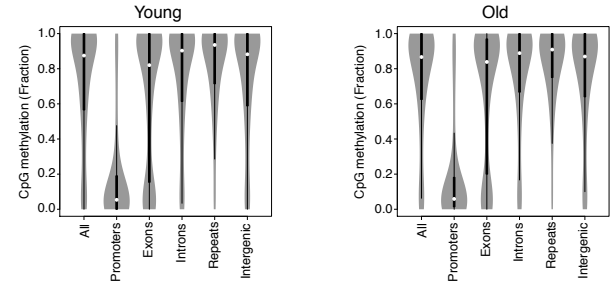

Supplemental Figure S3

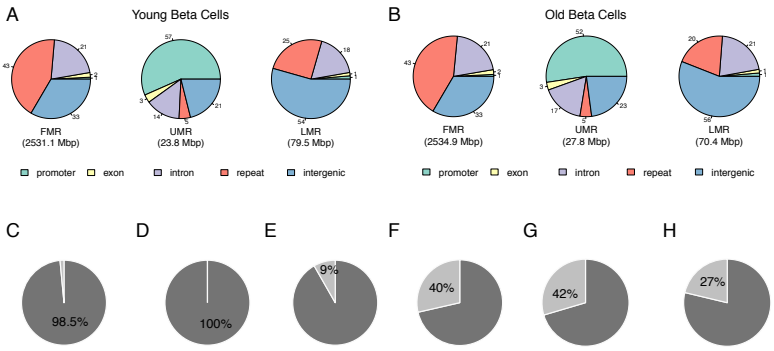

Supplemental Figure S4

Gene	Function	% increased methylation with age	p value (DMR)	Distance from TSS (bp)	Decreased expression With age (FC)	p value (RNA)
Anln	Anillin, required for cytokinesis	3.4	1.9E-18	160	15.4	0.0017
Mki67	cell proliferation	3.7	5.2E-18	-141	145.9	0.0000
Aurkb	Serine/threonine-protein kinase, regulation of mitosis	4.9	5.5E-08	241	24.3	0.0008
Cdca2	Regulator of chromosome structure during mitosis	2.4	1.3E-08	-116	21.3	0.0004
Cdca5	Regulator of sister chromatid cohesion in mitosis	5.4	1.2E-30	110	19.1	0.0016
Gsg2	cell cycle pregression	2.5	1.0E-12	199	135.3	0.0000
Mapk12	MAP kinase pathway, supports mitotic cell viability	4.9	3.0E-16	211	7.0	0.0075
Plk1	critical regulator of cell cycle progression	4	8.3E-10	224	21.5	0.0025
Ccnd3	Cyclin D3, regulators of CDK kinases, cell cycle progression	5.6	1.6E-24	605	2.3	0.0273
Ccna1	Cyclin A1, cell cycle control	3.6	1.2E-09	-247	20.2	0.0098
Fosb	TF complex AP-1, potential regulator of cell proliferation	3.8	3.8E-09	605	3.2	0.0024

Supplemental Figure S5

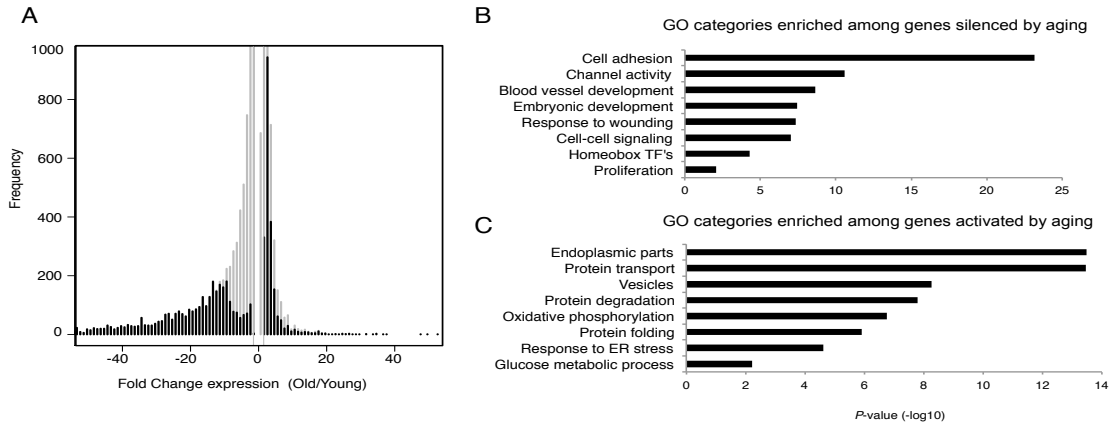

Supplemental Figure S6